Cache Placement in Fog-RANs:
From Centralized to Distributed Algorithms

Juan Liu, *Member, IEEE*, Bo Bai, *Member, IEEE*, Jun Zhang, *Senior Member, IEEE*,
and Khaled B. Letaief, *Fellow, IEEE*

Abstract—To deal with the rapid growth of high-speed and/or ultra-low latency data traffic for massive mobile users, fog radio access networks (Fog-RANs) have emerged as a promising architecture for next-generation wireless networks. In Fog-RANs, the edge nodes and user terminals possess storage, computation and communication functionalities to various degrees, which provides high flexibility for network operation, i.e., from fully centralized to fully distributed operation. In this paper, we study the cache placement problem in Fog-RANs, by taking into account flexible physical-layer transmission schemes and diverse content preferences of different users. We develop both centralized and distributed transmission aware cache placement strategies to minimize users' average download delay subject to the storage capacity constraints. In the centralized mode, the cache placement problem is transformed into a matroid constrained submodular maximization problem, and an approximation algorithm is proposed to find a solution within a constant factor to the optimum. In the distributed mode, a belief propagation based distributed algorithm is proposed to provide a suboptimal solution, with iterative updates at each BS based on locally collected information. Simulation results show that by exploiting caching and cooperation gains, the proposed transmission aware caching algorithms can greatly reduce the users' average download delay.

Index Terms—Content placement, Fog-RAN, submodular optimization, belief propagation.

I. INTRODUCTION

With the explosive growth of consumer-oriented multimedia applications, a large scale of end devices, such as smart phones, wearable devices and vehicles, need to be connected via wireless networking [2]. This has triggered the rapid increase of high-speed and/or ultra-low latency data traffic that is very likely generated, processed and consumed locally at the edge of wireless networks. To cope with this trend, fog radio access network (Fog-RAN) is emerging as a promising network architecture, in which the storage, computation, and

communication functionalities are moved to the edge of wireless networks, i.e., to the near-user edge devices and end-user terminals [2]–[4]. To further improve the delivery rate and decrease latency for mobile users, a promising solution is to push the popular contents towards end users by caching them at the edge nodes in Fog-RANs [3]. Thus, the content delivery service of mobile users consists of two phases, i.e., *cache placement* and *content delivery* [1], [5]–[9]. The recent works studying cache-aided wireless networks fall into two major categories: 1) analyzing the content delivery performance for certain cache placement policies; 2) designing cache placement strategies for efficient content delivery.

It is critical to study the content delivery performance in cache-assisted wireless networks to reveal the benefits of placing caches distributedly across the whole network [10]–[16]. By coupling physical-layer transmission and random caching, the authors in [10] investigated the system performance in terms of the average delivery rate and outage probability for small-cell networks, where cache-enabled BSs are modeled as a Poisson point process. In [11] and [12], the throughput-outage tradeoff was investigated and the throughput-outage scaling laws were revealed for cache-assisted wireless networks, where clustered device caching and one-hop device-to-device (D2D) transmission are applied. This line of works have also been extended to the multi-hop D2D network in [13], where the multi-hop capacity scaling laws were studied. The throughput scaling laws were studied for wireless Ad-Hoc networks with device caching in [14], where the maximum distance separable (MDS) code and cache-assisted multi-hop transmission/cache-induced coordinate multipoint (CoMP) delivery were applied. In [15] and [16], content-centric multicasting was studied for cache-enabled cloud RAN and heterogeneous cellular networks, respectively.

Cache placement strategies should be carefully designed such that flexible transmission opportunities can be provided among users and caching gain can be efficiently exploited in the content delivery phase [1], [7]–[9], [17]–[24]. The cache placement problem in femtocell networks was studied in [8], where femtocell BSs with finite-capacity storages are deployed to act as helper nodes to cache popular files. In [7], [17], coded caching was exploited to create simultaneous coded multicasting opportunities to mobile users. This work was extended to the decentralized setting in [18] and hierarchical two-layer network in [19], respectively. By applying an Alternating Direction Method of Multipliers approach, the authors of [21] proposed a distributed caching algorithm for cache-enabled small base stations (SBSs) to minimize the global backhaul

costs of all the SBSs subject to the cache storage capacities. In [9], the design of optimal cache placement was pursued for wireless networks, by taking the extra delay induced via backhaul links and physical-layer transmissions into consideration. The authors in [20] proposed user preference profile based caching policies for radio access networks along with backhaul and wireless channel scheduler to support more concurrent video sessions. In [22], mobility-aware caching strategies were proposed to exploit user mobility patterns to improve cache performance. The joint routing and caching problem was studied for small-cell networks and heterogeneous networks in [23] and [24], respectively, subject to both the storage and transmission bandwidth capacity constraints on the small-cell BSs.

The existing works mainly focused on designing centralized cache placement strategies for specific network structures (e.g. small cell networks), where some specific transmission schemes are applied for content delivery. However, very few works have studied the cache placement problem in Fog-RANs. We notice that different users may be connected to Fog-RANs in different ways and with different transmission opportunities. Meanwhile, Fog-RANs support flexible network operation, i.e., from fully centralized to fully distributed operation. This motivates us to develop both centralized and distributed transmission aware cache placement strategies for the emerging Fog-RANs so that the spectrum efficiency of content delivery is improved as much as possible.

In this paper, we consider a Fog-RAN system, where each user is served by one or multiple network edge devices, e.g., base stations (BSs), and each BS is equipped with a cache of finite capacity. In contrast to [8] and [24] where each user has the same file preference and file delivery scheme, we consider that the users have different file preferences [25] and possibly different candidate transmission schemes. Then, we formulate an optimization problem to minimize the users' average download delay subject to the BSs' storage capacities, which turns out to be NP-hard. To deal with this difficulty, we apply different optimization techniques to find efficient cache placement policies for centralized and distributed operation modes of Fog-RANs, respectively.

In the centralized mode, we transform the delay minimization problem into a matroid constrained submodular maximization problem [26]. In this problem, the average delay function is submodular for all the possible transmission schemes, and the cache placement strategy subject to the BSs' storage capacities is a partition matroid. Based on the submodular optimization theory [26], we then develop a centralized low-complexity algorithm to find a caching solution within $1/2$ of the optimum in polynomial-time complexity $\mathcal{O}(MNK)$, where M, N and K denote the number of BSs, files and users, respectively.

In the distributed mode, we develop a low-complexity belief propagation based distributed algorithm to find a suboptimal cache placement strategy [27]. Based on local information of its storage capacity, the users in its serving range and their file request statistics, each BS perform individual computation and exchange its belief on the local caching strategy with its neighboring BSs iteratively. Through iterations, the distributed
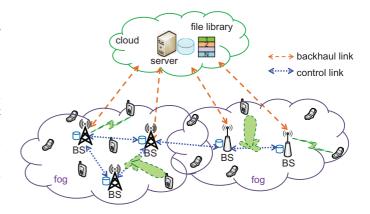

Fig. 1. An illustration of a Fog-RAN that consists of BSs and mobile users, where BSs are connected to a cloud data center via backhaul links. With the aid of transmission aware caching designs, the neighboring BSs could cache the same files and deliver them to their common users via cooperative beamforming.

algorithm converges to a suboptimal caching solution which achieves an average delay performance comparable to the centralized algorithm, as shown by simulation results. By distributing computing tasks, each individual BS always does much fewer calculations than the central controller when running the caching algorithms. Notice that the distributed caching algorithm proposed in [21] is run by each SBS individually and no parameters are shared between the SBSs. In this work, we propose a belief propagation based transmission aware distributed caching algorithm which requires cooperation and message passing between neighboring BSs.

The rest of this paper is organized as follows. Section II introduces the system model of Fog-RANs. Section III formulates the cache placement problem which minimizes the average download delay under the cache capacity constraints. In Section IV, a centralized algorithm is proposed to solve the cache placement problem under the framework of submodular optimization for the centralized Fog-RANs. In Section V, a belief propagation based distributed algorithm is proposed for cache placement in the distributed Fog-RANs. Section VI demonstrates the simulation results. Finally, Section VII concludes this paper.

II. SYSTEM MODEL

As shown in Fig. 1, we consider a Fog-RAN consisting of M edge nodes, i.e., BSs, and K mobile users. Let $\mathcal{A} = \{a_1, \cdots, a_M\}$ and $\mathcal{U} = \{u_1, \cdots, u_K\}$ denote the BS set and the user set, respectively. Each user can be served by one or multiple BSs, depending on the way it connects to the Fog-RAN. The connectivity between the users and the BSs is denoted by a $K \times M$ matrix $\boldsymbol{L}$, where each binary element l_{km} indicates whether user u_k can be served by BS a_m. That is, $l_{km} = 1$ if user u_k is located in the coverage of BS a_m, and $l_{km} = 0$ otherwise. The set of users in the coverage of BS a_m is denoted by $\mathcal{U}_m = \{u_k \in \mathcal{U} | l_{km} = 1\}$. Similarly, the set of serving BSs of user u_k is denoted by $\mathcal{A}_k = \{a_m \in \mathcal{A} | l_{km} = 1\}$.

Suppose that the library of N files, denoted by $\mathcal{F} = \{f_1, \cdots, f_N\}$, is stored at one or multiple content servers

which could be far away in the cloud data center. The content servers can be accessed by the BSs via backhaul links, as illustrated in Fig. 1. Assume all the files have the same size, i.e., $|f_n| = |f|$ ($\forall f_n \in \mathcal{F}$). The file popularity distribution conditioned on the event that user u_k makes a request is denoted by p_{nk}, which can be viewed as the user preference indicator and estimated via some learning procedure [28], [29]. The user's file preferences are normalized such that $\sum_{n=1}^{N} p_{nk} = 1$. We also assume that each BS a_m has a finite-capacity storage. Denote by Q_m the normalized storage capacity of BS a_m, which means that each BS a_m can store at most Q_m files. Let x_{nm} be a binary variable indicating whether file f_n is cached at BS a_m. That is, $x_{nm} = 1$ if file f_n is stored at BS a_m, and otherwise $x_{nm} = 0$. The caching variables $\{x_{nm}\}$ shall be determined collaboratively by the BSs to improve the probability that the users' requested files can be found in the caches of the BSs, i.e., the hit probability. Meanwhile, the cooperative caching strategy, denoted by $\boldsymbol{X}$, should also be carefully designed to provide flexible and cooperative transmission opportunities for each user.

When user u_k makes a request for file f_n, the serving BSs $\mathcal{A}_k$ jointly decide how to transmit to this user based on the caching strategy $\boldsymbol{X}$. Specifically, when file f_n is cached in one or multiple BSs, the BSs transmit this file to the user directly by employing some transmission schemes, e.g., non-cooperative transmission or cooperative beamforming, as shown in Fig. 1. When file f_n has not been cached in any serving BS of the user, the associated BSs $\mathcal{A}_k$ fetch the file from a content server via backhaul links before they transmit to user u_k over wireless channels.

The users' file delivery performance depends not only on the cache placement strategy but also on the specific transmission schemes applied to deliver the files to the users. In the following, we discuss the file delivery rates for some typical physical-layer transmission schemes, when the requested file is cached in one or multiple associated BSs.

1) Non-cooperative Transmission: When user u_k is served by one single BS a_m, a non-cooperative transmission scheme be applied by this BS to transmit the file to the user directly, if the requested file f_n is cached in this BS. Assume that efficient interference management schemes are applied and interference power is constrained by a fixed value χ. Let $\text{SINR}_m = \frac{P_m}{N_0 B + \chi}$ denote the target signal-to-interference-plus-noise ratio (SINR) at the transmitter side, where P_m is the average transmission power at BS a_m, N_0 is the power spectral density of noise, and B is the system bandwidth. The file delivery rate in time slot i can be estimated as

$$R_{nk}(\boldsymbol{X}, i) = B \log \left(1 + |h_{km}(i)|^2 l_{km} x_{nm} \text{SINR}_m \right), \quad (1)$$

where $h_{km}(i)$ denotes the channel coefficient between user u_k and BS a_m in time slot i.

2) Cooperative Beamforming: When user u_k is served by multiple BSs, cooperative beamforming can be applied by the associated BSs $\mathcal{A}_k$, if file f_n has been cached in multiple BSs and the instantaneous channel state information is available. During the file delivery phase, cooperative beamformer can be created possibly in a distributed way to avoid signaling

overhead [30]. Accordingly, the file delivery rate in time slot i is estimated as

$$R_{nk}(\boldsymbol{X}, i) = B \log \left(1 + \sum_{a_m \in \mathcal{A}_{k,n}} |h_{km}(i)|^2 x_{nm} \text{SINR}_m \right), \quad (2)$$

where $\mathcal{A}_{k,n} \subseteq \mathcal{A}_k$ denotes a set of BSs that transmit file f_n to user u_k via cooperative beamforming.

In this work, we aim at finding the optimal cache placement strategy to minimize the average download delay, considering different candidate transmission schemes for each user, as be presented in the next section.

III. PROBLEM FORMULATION FOR CACHE PLACEMENT

In this section, we first show how to calculate the average download delay by applying martingale theory [31]. Then, we formulate the cache placement problem.

Let $\bar{D}_{nk}(\boldsymbol{X})$ denote the average delay for user u_k to download file f_n from its serving BSs for a given caching strategy $\boldsymbol{X}$ and a specific transmission scheme. When file f_n has been cached in one or multiple BSs, user u_k can download this file from the associated BSs with rate $R_{nk}(\boldsymbol{X}, i)$ (c.f. (1)-(2)) in each time slot i. In this case, it takes at least $T_{nk}^*(\boldsymbol{X})$ time slots for user u_k to successfully receive all the bits of file f_n. The minimum number of time slots $T_{nk}^*(\boldsymbol{X})$ can be evaluated as

$$T_{nk}^*(\boldsymbol{X}) = \arg\min \left\{ T : \sum_{i=1}^{T} R_{nk}(\boldsymbol{X}, i) \geq \frac{|f_n|}{\Delta t} \right\}, \quad (3)$$

where Δt is the duration of one time slot. Thus, for user u_k, the average delay of downloading file f_n is expressed as

$$\bar{D}_{nk}(\boldsymbol{X}) = \mathbb{E}_{\boldsymbol{h}} \{ T_{nk}^*(\boldsymbol{X}) \} \Delta t. \quad (4)$$

When file f_n has not been cached at any associated BS, one or multiple serving BSs of user u_k, denoted by $\mathcal{A}_k'$, should first fetch the file from the content server via the backhaul link before delivering the requested file to this user over wireless channel. Let D_{nk} denote the extra delay of downloading file f_n from the content server to the BSs $\mathcal{A}_k'$. We then evaluate the average download delay under the assumption that the channel coefficients $\{h_{km}(i)\}$ are identically and independently distributed (i.i.d.) across the time slots i in the following theorem.

Theorem 1. *If the channel coefficients $\{h_{km}(i)\}$ are i.i.d. across the time slots, the average delay for user u_k to download file f_n can be expressed as*

$$\bar{D}_{nk}(\boldsymbol{X}) = \begin{cases} \frac{|f_n|}{\mathbb{E}_{\boldsymbol{h}} \{ R_{nk}(\boldsymbol{X}) \}}, & \sum_{a_m \in \mathcal{A}_k} x_{nm} \neq 0, \\ D_{nk} + \frac{|f_n|}{\mathbb{E}_{\boldsymbol{h}} \{ R_{nk}(\boldsymbol{X}_k) \}}, & \sum_{a_m \in \mathcal{A}_k} x_{nm} = 0. \end{cases}$$

(5)

where $\mathbb{E}_{\boldsymbol{h}} \{\cdot\}$ denotes the expectation over the channel coefficients $\{h_{km}(i)\}$ and $\boldsymbol{X}_k$ is a caching strategy with $x_{nm} = 1$ for $a_m \in \mathcal{A}_k'$.

Proof: The proof is deferred to Appendix A. ∎

From this theorem, we can evaluate the average download delay by (5) for any given caching strategy and employed

transmission scheme. Without loss of generality, we assume that the users' average delay of downloading file f_n from the content server is larger than the average delay of direct file delivery from the BSs and the following inequality holds:

$$\frac{|f_n|}{\mathbb{E}_{\boldsymbol{h}}\{R_{nk}(\boldsymbol{X}_k)\}} + D_{nk} > \max_{\sum_{a_m \in \mathcal{A}_k} x_{nm} \neq 0} \left\{ \frac{|f_n|}{\mathbb{E}_{\boldsymbol{h}}\{R_{nk}(\boldsymbol{X})\}} \right\}. \tag{6}$$

If D_{nk} is much larger than $\frac{|f_n|}{\mathbb{E}_{\boldsymbol{h}}\{R_{nk}(\boldsymbol{X}_k)\}}$, the average delay $\bar{D}_{nk}(\boldsymbol{X})$ can be approximated by D_{nk} when $\sum_{a_m \in \mathcal{A}_k} x_{nm} = 0$. Notice that D_{nk} is the sum of the delay of file delivery within the Internet which mainly depends on the level of congestion in the network, and the delay of file delivery via backhaul links which may depend on the backhaul capacities and the caching strategy $\boldsymbol{X}$. Considering all these effects, the impact of the caching strategy $\boldsymbol{X}$ on the delay D_{nk} is negligible. Hence, we assume that the average delay D_{nk} is fixed and can be evaluated by the average time of downloading file f_n from the content server to the serving BSs of user u_k.

In the considered system, we seek to design transmission aware cache placement strategies to minimize the average delay of all the users, by taking different candidate transmission schemes for each user into consideration. Formally, the cache placement problem can be formulated as follows

$$\begin{aligned} \underset{\{x_{nm}\}}{\text{minimize}} \quad & \bar{D}(\boldsymbol{X}) = \frac{1}{K}\sum_{k=1}^{K}\sum_{n=1}^{N} p_{nk}\bar{D}_{nk}(\boldsymbol{X}) \\ \text{subject to} \quad & \begin{cases} \sum_{n=1}^{N} x_{nm} \leq Q_m, \forall a_m \in \mathcal{A}, & (a) \\ x_{nm} \in \{0,1\}, \forall f_n \in \mathcal{F}, a_m \in \mathcal{A}, & (b) \end{cases} \end{aligned} \tag{7}$$

where constraint (7.a) means that each BS a_m is allowed to store at most Q_m files. Since the variable x_{nm} is binary, Problem (7) is a constrained integer programming problem, which is generally NP-hard [32]. Hence, it is very challenging to find the optimal solution $\boldsymbol{X}^*$ to Problem (7). In the next two sections, we show how to approach the optimal cache placement strategy in the centralized and distributed modes of Fog-RANs, respectively.

IV. SUBMODULAR OPTIMIZATION BASED CENTRALIZED CACHE PLACEMENT ALGORITHM

As a powerful tool for solving combinatorial optimization problems, the submodular optimization is applied when Fog-RANs operate in the centralized mode with the aid of a central controller. In this section, Problem (7) is first reformulated into a monotone submodular optimization problem subject to a matroid constraint. A centralized low-complexity greedy algorithm is then proposed to obtain a suboptimal cache placement strategy with guaranteed performance. The basic concepts about matroid and submodular function can be found in [26].

A. Matroid Constrained Submodular Optimization

We first define the ground set for cache placement as

$$\mathcal{S} = \left\{ f_1^{(1)}, \cdots, f_N^{(1)}, \cdots, f_1^{(M)}, \cdots, f_N^{(M)} \right\}, \tag{8}$$

where $f_n^{(m)}$ denotes the event that file f_n is placed in the cache of BS a_m. The ground set $\mathcal{S}$ contains all possible caching strategies which can be applied in the system. In particular, we use

$$\mathcal{S}_m = \left\{ f_1^{(m)}, f_2^{(m)}, \cdots, f_N^{(m)} \right\} (\forall m = 1, 2, \ldots, M) \tag{9}$$

to denote the set of all files that might be placed in the cache of BS a_m. Thus, the ground set $\mathcal{S}$ can be partitioned into M disjoint sets, i.e., $\mathcal{S} = \bigcup_{m=1}^{M} \mathcal{S}_m$, $\mathcal{S}_m \bigcap \mathcal{S}_{m'} = \emptyset$ for any $m \neq m'$.

Given the finite ground set $\mathcal{S}$, we continue to define a partition matroid $\mathcal{M} = (\mathcal{S}; \mathcal{I})$, where $\mathcal{I} \subseteq 2^{\mathcal{S}}$ is a collection of independent sets defined as:

$$\mathcal{I} = \left\{ \mathcal{X} \subseteq \mathcal{S} : \left| \mathcal{X} \bigcap \mathcal{S}_m \right| \leq Q_m, \forall m = 1, 2, \ldots, M \right\}, \tag{10}$$

which accounts for the constraint on the cache capacity Q_m at each BS a_m (c.f. (7.a)). The set of files placed in the cache of BS a_m can be denoted by $\mathcal{X}_m = \mathcal{X} \bigcap \mathcal{S}_m$.

Then, we show that the average delay is a monotone supermodular set function over the ground set $\mathcal{S}$. Note that every set has an equivalent boolean presentation. For any $\mathcal{X} \subseteq \mathcal{S}$, the incidence vector of $\mathcal{X}$ is denoted by the vector $\boldsymbol{\mu} \in \{0,1\}^{\mathcal{S}}$ whose i-th element is defined as

$$\mu_i \doteq x_{nm}, \quad i = (m-1)N + n, \tag{11}$$

where $\doteq$ represents the mapping between x_{nm} and μ_i. In the set $\mathcal{X} \subseteq \mathcal{S}$, $f_n^{(m)} \in \mathcal{X}$ indicates $\mu_i = x_{nm} = 1$. Otherwise, $\mu_i = x_{nm} = 0$. Similarly, the boolean presentation of the subset $\mathcal{X}_m$ is denoted by $\boldsymbol{\mu}_m$. In this context, the delay function $\bar{D}_{nk}(\boldsymbol{X})$ is equivalent to the set function $\bar{D}_{nk}(\mathcal{X})$ over the set $\mathcal{X} \subseteq \mathcal{S}$. The property of $\bar{D}_{nk}(\mathcal{X})$ is summarized in the following theorem.

Theorem 2. $\tilde{D}_{nk}(\mathcal{X}) = -\bar{D}_{nk}(\mathcal{X})$ *is a monotone submodular function defined over* $\mathcal{X} \in \mathcal{I}$.

Proof: The proof is deferred to Appendix B. ∎

From [26], the class of submodular functions is closed under non-negative linear combinations. Therefore, for $p_{nk} \geq 0$ with $k = 1, 2, \ldots, K$ and $n = 1, 2, \ldots, N$, the set function

$$\tilde{D}(\mathcal{X}) = \frac{1}{K}\sum_{k=1}^{K}\sum_{n=1}^{N} p_{nk}\tilde{D}_{nk}(\mathcal{X}) \tag{12}$$

is also monotone submodular.

By taking the partition matroid $\mathcal{M} = (\mathcal{S}; \mathcal{I})$ (c.f. (10)) into consideration, Problem (7) can be reformulated into a matroid constrained monotone submodular maximization problem:

$$\begin{aligned} \text{maximize} \quad & \tilde{D}(\mathcal{X}) = \frac{1}{K}\sum_{k=1}^{K}\sum_{n=1}^{N} p_{kn}\tilde{D}(\mathcal{X}) \\ \text{subject to} \quad & \mathcal{X} \in \mathcal{I}, \end{aligned} \tag{13}$$

where the constraint $\mathcal{X} \in \mathcal{I}$ (c.f. (10)) shows that each BS a_m can cache up to Q_m files.

Algorithm 1 Centralized algorithm for cache placement

1: Set $\mathcal{X} \leftarrow \emptyset$ and $\mathcal{Y} \leftarrow \mathcal{S}$;
2: Set $\mathcal{X}_m \leftarrow \emptyset$ and $\mathcal{Y}_m \leftarrow \mathcal{S}_m$ for $m = 1, 2, \cdots, M$;
3: Calculate $\Delta_{\mathcal{X}}(s)$ for each element $s \in \mathcal{S} \backslash \mathcal{X}$;
4: **repeat**
5:    Select the element $f_n^{(m)}$ with the highest marginal gain,
$$f_n^{(m)} = \arg \max_{s \in \mathcal{S} \backslash \mathcal{X}, \mathcal{X} \bigcup \{s\} \in \mathcal{I}} \Delta_{\mathcal{X}}(s);$$
6:    Add $f_n^{(m)}$ to the sets $\mathcal{X}$ and $\mathcal{X}_m$:
$$\mathcal{X} \leftarrow \mathcal{X} \bigcup \{f_n^{(m)}\}, \mathcal{X}_m \leftarrow \mathcal{X}_m \bigcup \{f_n^{(m)}\};$$
7:    Remove $f_n^{(m)}$ from the sets $\mathcal{Y}$ and $\mathcal{Y}_m$:
$$\mathcal{Y}_m \leftarrow \mathcal{Y}_m \backslash \{f_n^{(m)}\}, \mathcal{Y} \leftarrow \mathcal{Y} \backslash \{f_n^{(m)}\};$$
8:    **if** $|\mathcal{X}_m| = Q_m$ **then**
9:       $\mathcal{Y} \leftarrow \mathcal{Y} \backslash \mathcal{Y}_m$;
10:    **end if**
11:    Calculate $\Delta_{\mathcal{X}}(s)$ for each element $s \in \mathcal{S} \backslash \mathcal{X}$;
12: **until** $\mathcal{Y} = \emptyset$ or $\Delta_{\mathcal{X}}(s) = 0$ for all $s \in \mathcal{S} \backslash \mathcal{X}$

B. Centralized Algorithm Design for Cache Placement

We adopt a greedy algorithm [26] to find a suboptimal solution to Problem (13) in a centralized way. Define the marginal gain of adding one element $s \in \mathcal{S} \backslash \mathcal{X}$ to the set $\mathcal{X}$ as

$$\Delta_{\mathcal{X}}(s) = \tilde{D}\left(\mathcal{X} \bigcup \{s\}\right) - \tilde{D}(\mathcal{X}). \tag{14}$$

At first, $\mathcal{X}$ and $\mathcal{X}_m$ are initialized to be the empty set $\emptyset$, while $\mathcal{Y}$ and $\mathcal{Y}_m$ are initialized as the set $\mathcal{S}$. In each step, we calculate the marginal gain $\Delta_{\mathcal{X}}(s)$ for each element $s \in \mathcal{S} \backslash \mathcal{X}$ and select the element $f_n^{(m)}$ with the highest marginal gain, i.e.,

$$f_n^{(m)} = \arg \max_{s \in \mathcal{S} \backslash \mathcal{X}, \mathcal{X} \bigcup \{s\} \in \mathcal{I}} \Delta_{\mathcal{X}}(s), \tag{15}$$

where $\mathcal{X} \bigcup \{s\} \in \mathcal{I}$ indicates that adding the new element $f_n^{(m)}$ into the current set $\mathcal{X}$ does not violate the cache capacity constraint at each BS a_m. Then, we add this element $f_n^{(m)}$ to the set $\mathcal{X}_m$ as well as the set $\mathcal{X}$, and remove it from the sets $\mathcal{Y}$ and $\mathcal{Y}_m$ at the same time. When the set $\mathcal{X}_m$ has accumulated Q_m elements, the set $\mathcal{Y}_m$ be removed from the set $\mathcal{Y}$, which means that BS a_m has cached up to Q_m files and has no space for any more file. This step runs repeatedly until no more element can be added, i.e., the marginal value $\Delta_{\mathcal{X}}(s)$ is zero for all $s \in \mathcal{S} \backslash \mathcal{X}$ or the set $\mathcal{Y}$ becomes empty. The above procedures are summarized in Algorithm 1. According to [33], the greedy algorithm can achieve the expected $1/2$-ratio of the optimal value in general. The computation complexity of the centralized algorithm can be estimated as $\mathcal{O}(NMK)$ in the worst case.

V. BELIEF PROPAGATION BASED DISTRIBUTED CACHE PLACEMENT ALGORITHM

When Fog-RANs operate in the distributed mode, there exists no central controller. The BSs should carry out a distributed algorithm for cache placement autonomously, relying on locally collected network-side and user-related information, as well as local interactions between BSs in the neighborhood. In this section, we propose a belief propagation based distributed algorithm to perform cooperative caching. The basic

concept of the message passing procedure can be found in Appendix C.

A. Factor Graph Model for Cache Placement

To apply the belief propagation based distributed algorithm, Problem (7) is first transformed into an unconstrained optimization problem as presented in Lemma 3. To this end, we define two functions of the caching strategy $\boldsymbol{X}$ as:

$$\eta_{nk}(\boldsymbol{X}) = \exp\left(-p_{nk}\bar{D}_{nk}(\boldsymbol{X})\right), \tag{16}$$

$$g_m(\boldsymbol{X}) = \begin{cases} 1, & \sum_{n=1}^{N} x_{nm} \leq Q_m, \\ 0, & \text{otherwise.} \end{cases} \tag{17}$$

Lemma 3. *Let $\mathcal{C} = \{(f_n, u_k) | p_{nk} > 0, f_n \in \mathcal{F}, u_k \in \mathcal{U}\}$ denote the set of all possible pairs of file f_n and user u_k. Problem (7) is equivalent to the following problem*

$$\hat{\boldsymbol{X}} = \arg \max_{\boldsymbol{X} \in \{0,1\}^{NM}} \prod_{(f_n, u_k) \in \mathcal{C}} \eta_{nk}(\boldsymbol{X}) \prod_{m=1}^{M} g_m(\boldsymbol{X}). \tag{18}$$

Proof: Problem (7) is equivalent to maximizing $-\sum_{k=1}^{K} \sum_{n=1}^{N} p_{nk} \bar{D}_{nk}(\boldsymbol{X})$ subject to the constraints $\sum_{n=1}^{N} x_{nm} \leq Q_m$ for all m. By introducing the exponential function $\eta_{nk}(\boldsymbol{X})$ given by (16) and the indicator function $g_m(\boldsymbol{X})$ given by (17), the equivalent optimization problem is converted into a product form, as presented in (18). ∎

In (18), $\eta_{nk}(\boldsymbol{X})$ is used to measure the delay performance when transmitting file f_n to user u_k, and $g_m(\boldsymbol{X})$ imposes a strict constraint on the cache capacity of BS a_m.

Then, we present the factor graph model for the optimization problem (18). According to the network topology (e.g., Fig. 2(a)), we introduce a variable node μ_i for each element x_{nm} and a function node F_j for each function $\eta_{nk}(\boldsymbol{X})$ or $g_m(\boldsymbol{X})$, as shown in Fig. 2(b). The mapping rule from x_{nm} to μ_i is given by (11), and the mapping rule from $\eta_{nk}(\boldsymbol{X})$ or $g_m(\boldsymbol{X})$ to F_j is expressed as
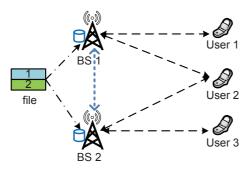
$$F_j \doteq \begin{cases} \eta_{nk}, & j = \sum_{l=1}^{k-1} |\mathcal{F}_l| + \xi(n,k), \\ g_m, & j = \sum_{k=1}^{K} |\mathcal{F}_k| + m, \end{cases} \tag{19}$$

where $\mathcal{F}_k = \{f_n | p_{nk} > 0\}$ denotes the set of files which may be requested by user u_k, and $|\mathcal{F}_k|$ is the number of elements in the set $\mathcal{F}_k$, and $\xi(n,k)$ denotes the index of file f_n in the set $\mathcal{F}_k$.
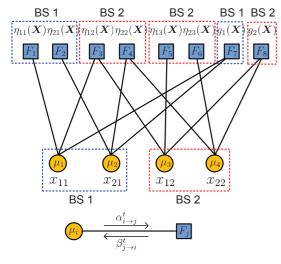
In the bipartite factor graph (e.g., Fig. 2(b)), each variable node $\mu_i \doteq x_{nm}$ is adjacent to the function nodes $\{F_j\} \doteq \{\eta_{nk}\} \bigcup \{g_m\}$ for all $u_k \in \mathcal{U}_m$. Similarly, each function node $F_j \doteq \eta_{nk}$ is connected to the variable nodes $\{\mu_i = x_{nm}\}$ for all $a_m \in \mathcal{A}_k$. Each function node $F_j \doteq g_m$ is adjacent to the variable nodes $\{\mu_i \doteq x_{nm}\}$ for all $f_n \in \mathcal{F}$. Hence, there are $I = NM$ variable nodes and $J = M + \sum_{k=1}^{K} |\mathcal{F}_k|$ function nodes in this factor graph model.

B. Message Passing Procedure for Cache Placement

Our goal is to design a message-passing procedure which allows us to gradually approach the optimal solution to (18).

(a) Connectivity between the BSs and users

(b) The factor graph model

Fig. 2. An illustrative example: (a) a system with 2 BSs, 3 users, and a library of 2 files, (b) the factor graph model.

1) Message Update : Let $m^t_{\mu_i \to F_j}(x)$ denote the message from a variable node μ_i to a function node F_j, and $m^t_{F_j \to \mu_i}(x)$ denote the message from a function node F_j to a variable node μ_i, respectively. The update of the messages $m^t_{\mu_i \to F_j}(x)$ and $m^t_{F_j \to \mu_i}(x)$ can be obtained by (31) and (32), respectively. Since all the variables $\{x_{nm}\}$ are binary, it is sufficient to pass the scalar ratio of the messages between each pair of nodes in practice. We can also express the message ratios in the logarithmic domain as

$$\alpha^t_{i \to j} = \log\left(\frac{m^t_{\mu_i \to F_j}(1)}{m^t_{\mu_i \to F_j}(0)}\right), \beta^t_{j \to i} = \log\left(\frac{m^t_{F_j \to \mu_i}(1)}{m^t_{F_j \to \mu_i}(0)}\right). \quad (20)$$

In this way, the computation complexity and communication overhead are greatly reduced. This is because only half of the messages are actually calculated and passed. As shown in Fig. 2(b), the message $\alpha^t_{i \to j}$, instead of $m^t_{\mu_i \to F_j}(x)$ ($x \in \{0,1\}$), is sent from the variable node μ_i to the function node F_j, and the message $\beta^t_{j \to i}$, instead of $m^t_{F_j \to \mu_i}(x)$ ($x \in \{0,1\}$), is sent from the function node F_j to the variable node μ_i. Meanwhile, the product operations in (31) and (32) become simple additive operations in the logarithmic domain, as presented in the following theorem.

Theorem 4. *The message $\alpha^t_{i \to j}$ is updated as*

$$\alpha^{t+1}_{i \to j} = \sum_{l \in \Gamma^\mu_i \setminus \{j\}} \beta^t_{l \to i}. \quad (21)$$

When $F_j \doteq \eta_{nk}$, the message $\beta^{t+1}_{j \to i}$ is given by

$$\beta^{t+1}_{j \to i} = p_{nk}\left(\bar{D}_{nk}(\boldsymbol{X}^t_{i,0}) - \bar{D}_{nk}(\boldsymbol{X}^t_{i,1})\right), \quad (22)$$

where the caching vectors $\boldsymbol{X}^t_{i,0}$ and $\boldsymbol{X}^t_{i,1}$ can be obtained by assigning their elements as

$$x_{nm} \doteq \mu_l = \begin{cases} 1, & l \in E^t_i = \{i_1 \in \Gamma^F_j \setminus \{i\} | \alpha^t_{i_1 \to j} > 0\}, \\ 0, & otherwise, \end{cases}$$

and

$$x_{nm} \doteq \mu_l = \begin{cases} 1, & l \in E^t_i \bigcup \{i\}, \\ 0, & otherwise, \end{cases}$$

respectively. When $F_j \doteq g_m$, the message $\beta^t_{j \to i}$ is updated as

$$\beta^{t+1}_{j \to i} = \min\left\{0, -\alpha^{(Q_m)}_{l \to j}(t)\right\}, \quad (23)$$

where $\alpha^{(Q_m)}_{l \to j}(t)$ is the Q_m-th message among the messages $\{\alpha^t_{l \to j}\}$ ($l \in \Gamma^F_j \setminus \{i\}$) sorted in the descending order.

Proof: The proof is deferred to Appendix D. ∎

In practice, the messages $\alpha^t_{i \to j}$ and $\beta^t_{j \to i}$ reflect the beliefs on the value of μ_i and should be updated according to (21) and (22) (or (23)), respectively, in each iteration.

2) Belief Update : In the t-th iteration, the belief on $\mu_i = x$ is expressed as

$$b^{t+1}_i(x) = \prod_{j \in \Gamma^\mu_i} m^t_{F_j \to \mu_i}(x), \quad (24)$$

which is the product of all the messages incident to μ_i. Hence, the belief ratio in the logarithmic domain can be obtained as

$$\tilde{b}^t_i = \log\left(\frac{b^t_i(1)}{b^t_i(0)}\right) = \sum_{j \in \Gamma^\mu_i} \beta^t_{j \to i}, \quad (25)$$

where $\beta^t_{j \to i}$ is given by (23) for $F_l \doteq g_m$, and by (22) for $F_j \doteq \eta_{nk}$ ($j \in \Gamma^\mu_i \setminus \{l\}$), respectively. As a result, the estimation of μ_i can be expressed as

$$\hat{\mu}^t_i = \begin{cases} 1, & \text{if } \tilde{b}^t_i > 0, \\ 0, & \text{if } \tilde{b}^t_i < 0. \end{cases} \quad (26)$$

In each iteration, each variable node μ_i updates its belief on its associated variable x_{nm} according to (25) and makes an estimate of x_{nm} according to (26) until it converges.

C. Distributed Cache Placement Algorithm

When we map the message passing procedure derived on the factor graph (e.g., Fig. 2(b)) back to the original network graph (e.g., Fig. 2(a)), we notice that all the messages are updated at the BSs and some of them be exchanged between neighboring BSs.

Algorithm 2 Distributed algorithm for cache placement

1: Map η_{nk}, g_m to F_j and x_{nm} to μ_i for $\forall n, k, m$,
2: Set $t = 0$ and $\alpha_{i \rightarrow j}^t = \beta_{j \rightarrow i}^t = 0$, $\forall i, j$,
3: Set t_{max} as a sufficiently large constant.
4: **while** Not convergent and $t \leq t_{max}$ **do**
5:    **for** $m = 1 : M$ **do**
6:       **for** $n = 1 : N$ **do**
7:          Calculate the message $\alpha_{i \rightarrow j}^t$ by (21);
8:          **for** $k \in \widetilde{\mathcal{U}}_m$ **do**
9:             Calculate the message $\beta_{j \rightarrow i}^t$ for $F_j \doteq \eta_{nk}$ by (22);
10:          **end for**
11:       **end for**
12:       Calculate the message $\beta_{j \rightarrow i}^t$ for $F_j \doteq g_m$ by (23);
13:       Calculate the belief $\tilde{b}_i^t$ by (25);
14:       Estimate each variable $\hat{\mu}_i$ by (26);
15:    **end for**
16:    Check the convergence, and set $t = t + 1$;
17: **end while**
18: Obtain the optimal estimate $\hat{\boldsymbol{X}}$ to the solution of (18).
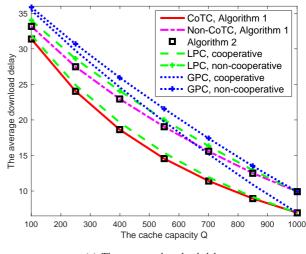
---

1) Scenario I: When user u_k is connected to one single BS a_m, as shown in Fig. 2(b), the update of messages $\alpha_{i \rightarrow j}^t$ and $\beta_{j \rightarrow i}^t$ is performed at this BS for the variable node $\mu_i \doteq x_{nm}$, the function nodes $F_j \doteq \eta_{nk}$, and $F_j \doteq g_m$. In this case, each BS a_m performs the message calculation and belief update for all the users just served by itself, i.e., $u_k \in \mathcal{U}_m$ and $|\mathcal{A}_k| = 1$.

2) Scenario II: When user u_k is in the coverage of multiple BSs $\mathcal{A}_k$, the update of messages $\alpha_{i \rightarrow j}^t$ and $\beta_{j \rightarrow i}^t$ associated with the function node $F_j \doteq \eta_{nk}$ is performed at one BS a_m and be exchanged between the serving BSs of this user $\mathcal{A}_k$ over control links, as shown in Fig. 1.
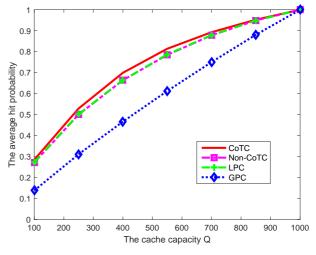
Notice that message exchanges just take place in Scenario II, and the communication overhead induced depends on the number of common users covered by multiple BSs. From the above discussion, we summarize the message passing based distributed algorithm for cache placement in Algorithm 2. In this algorithm, the message update for each user should be performed just once by one single BS in each iteration. To avoid confusion, $\widetilde{\mathcal{U}}_m$ is used to denote the set of users whose messages are processed by BS a_m in Algorithm 2.

VI. SIMULATION RESULTS

In this section, we present simulation results to demonstrate the performance of the proposed cache placement algorithms, i.e., Algorithm 1 and Algorithm 2. We consider a Fog-RAN with M BSs and K mobile users. Each BS serves the users in a circular cell with a radius of 150m, and the distance between neighboring BSs is 200m. K users are uniformly and independently distributed in the area covered by the M cells. File requests of each user u_k follow the Zipf distribution with parameter γ_k. The users in the cell interior are served by just one single BS, while the users in the overlapping area of cells are covered by multiple BSs and thus cooperative transmission may be enabled. The connectivity between the BSs and users is thus established.

(a) The average download delay

(b) The average hit probability

Fig. 3. The average delay and hit probability of the proposed caching strategies when $\gamma_k = 0.65$ and $N = 1000$.

Suppose that the system bandwidth is 5MHz, and the length of each time slot is 20ms. The file size is equal to 100Mbits. The path-loss exponent is set as 3.5. The small-scale channel gain $|h_{km}|^2$ follows independently standard exponential distribution in each time slot. Assume that no inter-cell interference is induced by adopting appropriate scheduling policies, and the transmit power is set to make sure that the average received SNR at the cell edge is equal to 0dB. Unless otherwise stated, we set $K = 100$, $M = 10$, and $D_{nk} = 40$s. Suppose that each user u_k requests file f_n with probability $p_{nk} = \frac{(\phi(n))^{-\gamma_k}}{\sum_{n=1}^{N} n^{-\gamma_k}}$, where $\{\phi(n)\}_{n=1}^{N}$ is a random permutation of $[1, \cdots, N]$, i.e., we assume different users have different request distributions.

In the considered system, we compare two transmission aware caching strategies and two baseline popular caching strategies: 1) Non-cooperative transmission aware caching (Non-CoTC) strategy, which is designed based on prior knowledge that each individual user has the file preference p_{nk} and is served by one serving BS using non-cooperative transmission

given by (1); 2) Cooperative transmission aware caching (CoTC) strategy, which is designed based on prior knowledge that each individual user has the file preference p_{nk} and is served by one BS using non-cooperative transmission given by (1), or by multiple BSs using cooperative beamforming given by (2), depending on the connectivity between the user and the BSs; 3) Globally popular caching (GPC) strategy, which caches the most Q_m popular files at each BS a_m based on the network-wide file popularity $\{\tilde{p}_n\}$. Here, the file popularity is evaluated as $\tilde{p}_n = \frac{1}{K}\sum_{k=1}^{K} p_{nk}$, i.e., the average value of the file preferences of users in the network; 4) Locally popular caching (LPC) strategy, which caches the most Q_m popular files at each BS a_m based on the local file popularity $\tilde{p}_n^{(m)} = \frac{1}{|\mathcal{U}_m|}\sum_{u_k \in \mathcal{U}_m} p_{nk}$, i.e., the average value of the file preferences of users served by the BS a_m. The proposed transmission aware caching strategies can be performed in either a centralized or a distributed way. There is no difference between centralized and distributed ways of performing the Popular caching strategy.

A. Performance Evaluation

We demonstrate the performances of our considered four caching strategies in two scenarios when $\gamma_k = 0.65$, $N = 1000$ and $\gamma_k = 0.2 + 4.8\frac{k}{K}$, $N = 200$ in Fig. 3 and Fig. 4, respectively. In each scenario, we plot the average download delay and hit probability curves of these caching strategies in sub-figures (a) and (b), respectively, for different cache capacities $Q_m = Q$. When our proposed Non-CoTC or CoTC strategy is applied, the users' average download delay $\bar{D}(\boldsymbol{X})$ is computed by substituting the solution $\boldsymbol{X}$ that is achieved either by Algorithm 1 or by Algorithm 2. When the GPC or LPC strategy is applied, the average delay $\bar{D}(\boldsymbol{X})$ is obtained by substituting the GPC or LPC solution $\boldsymbol{X}$. As shown in Fig. 3 and Fig. 4, the average download delay monotonically decreases with the increase of the cache capacity Q for any given caching strategy. This is due to the fact that with the increase of storage capacity, more files are cached in each BS and more users can download files from local BSs instead of the content server. Due to the same reason, the users' average hit probability monotonically increases with the cache capacity.

As shown in Fig. 3(a) and Fig. 4(a), the two transmission aware caching strategies, i.e., Non-CoTC and CoTC, achieve smaller average download delays than the two popular caching strategies, i.e., LPC and GPC, for any cache capacity Q less than N. Meanwhile, the average hit probabilities of the CoTC and Non-CoTC strategies are higher or equal to that of the LPC strategy, and much higher than the GPC strategies when $Q < N$, as shown in Fig. 3(b) and Fig. 4(b). This is because the transmission aware caching strategies cache files at the BSs based on the accurate file preferences of individual users and the prior information on content delivery techniques that will be applied by the BSs. While the LPC or GPC strategy performs caching based on the file preference statistics of the users in each cell or in the network, which could not reflect the file preferences of individual users.

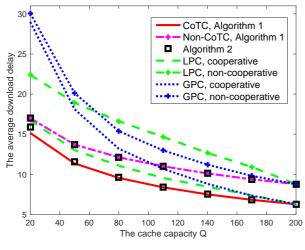The delay performance of the caching strategies not only depends on the users' hit performance, but also on the trans-mission schemes the BSs will adopt to deliver the requested files. It is observed from Fig. 3(a) and Fig. 4(a) that the CoTC strategy performs much better than the Non-CoTC strategy in terms of the average delay and hit probability. The delay performance gap between the two transmission aware caching strategies becomes larger as the cache capacity increases, since more files can be cached to facilitate cooperative transmission for cell-edge users. In other words, the CoTC strategy can exploit both caching gain and cooperative gain to reduce the average delay. Hence, the design of caching strategies should not only target at improving the users' average hit probability, but also bringing more cooperative transmission opportunities. Similarly, the delay performance is significantly improved when cooperative transmission is applied instead of non-cooperative transmission for any caching strategy.

At the same time, the users' skewness on content popularity has a great impact on the performances of the considered caching strategies. When $\gamma_k = 0.65$, each user is interested in a large number of files while only a very small number of files can be cached locally at the serving BSs of each user when Q is less than N. From Fig. 3(a), the delay gap between the CoTC (or Non-CoTC) strategy and the LPC strategy is not very large. And the GPC strategy which caches the same files in each BS achieves the worst delay and hit performances. When $\gamma_k = 0.2 + 4.8\frac{k}{K}$, the skewness on content popularity is quite different among users. This means some users have interests on many files while some users just have preferences on very few files. In contrast to the case with $\gamma_k = 0.65$, a higher proportion of the files that the users may request can be cached at the BSs. Therefore, the delay and hit performances of the considered caching strategies are all improved. And the delay gap between the CoTC (or Non-CoTC) strategy and the LPC strategy becomes very significant especially when the cache capacity Q is very small. It is also interesting to see that the delay performance of the LPC strategy gets affected by content delivery schemes applied by the BSs. As shown in Fig. 4(a), the LPC strategy always achieves a smaller average delay than the GPC strategy if cooperative transmission is adopted. However, it performs worse in the larger Q region ($Q > 65$) when non-cooperative transmission is applied. This happens when some users are served by their serving BSs which have not cached their requested files, since the LPC strategy caches files based on the file preferences of co-located users and pushes quite different contents in each BS.

From Fig. 3 and Fig. 4, the proposed belief propagation based distributed algorithm can achieve a nearly identical delay performance as compared to the centralized greedy algorithm which provides a guaranteed performance [33], i.e., $1/2$-approximation in the general case and $(1 - 1/e)$-approximation in some special cases. It has a slightly larger delay performance in the small-capacity region (e.g., Q is around 20), and achieves almost the same performance as the centralized algorithm in other scenarios.

B. Approximation of File Preferences

In practice, it is very challenging to accurately estimate the file preference of each individual user due to the lack
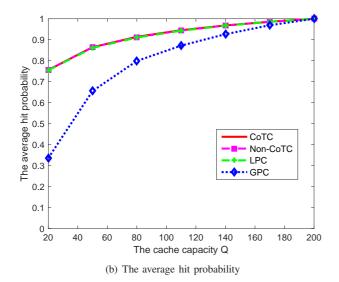
(a) The average download delay

(b) The average hit probability

Fig. 4. The average delay and hit probability performances of the proposed caching strategies when $\gamma_k = 0.2 + 4.8\frac{k}{K}$ and $N = 200$.
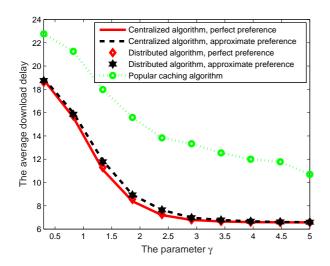

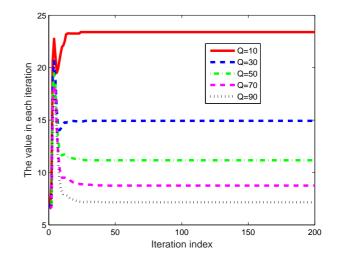Fig. 5. The average download delay vs. the parameter γ.

Fig. 6. The iterative procedure of the proposed distributed algorithm.

of sufficient samples. Instead, each BS may estimate an approximate file preference for all the users in its coverage, i.e., to estimate the average preference. In this part, we discuss the impact of the users' file request preference statistics, either perfectly or approximately known. In Fig. 5, we show how the average download delay changes with the content popularity skewness. In this experiment, all the users are supposed to have the same preference parameter $\gamma_k = \gamma$. The cache capacity is set as $Q = 50$ and the total number of files is $N = 100$. The approximate preference for file f_n is given by $\tilde{p}_{nk} = \frac{1}{|\mathcal{U}_m|} \sum_{u_k \in \mathcal{U}_m} p_{nk}$ ($\forall u_k \in \mathcal{U}_m$), i.e., only the statistical average of all the users in the coverage of each BS a_m is known, while a perfect knowledge p_{nk} includes preference for each individual user. It is observed that the average delay is significantly reduced when the parameter γ is increased within $0.3 \leq \gamma \leq 3$. In this range, the users have preferences on fewer and fewer files with the increase of the parameter γ. This means that more and more requested files are cached at the BSs, and can be transmitted to the users directly. As a result, the average download delay is greatly reduced when γ is increased within $0.3 \leq \gamma \leq 3$. When $\gamma > 3$, almost all the requested files have been cached and the average download delay is nearly equal to the average transmission time from the BSs to the users. In this case, the change of the average delay is not obvious. In Fig. 5, we also plot the average delay performance when approximate file preferences instead of accurate file preferences are applied. It can be seen that the delay gap is very small.

In Fig. 6, we plot the iterative procedure of the belief propagation based distributed algorithm for different storage capacities $Q_m = Q$ and $N = 100$. In this experiment, the CoTC strategy is performed in a distributed way. It is observed that the average delay starts from an initial value, fluctuates up to dozens of iterations and gradually converges to a suboptimal solution.
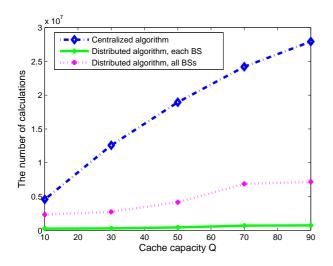
Fig. 7. The number of calculations vs. cache capacity Q.

C. Algorithm Complexity

We now discuss the computation complexity of our proposed centralized and distributed algorithms when performing the CoTC strategy. Here, we measure the computation complexity by the number of calculations required in the algorithms. In Fig. 7, we plot the computation complexity of the proposed algorithms versus the cache capacity Q. In this experiment, the number of BSs and the number of users are set as $M = 10$ and $K = 100$, and the total number of files is set to be 100. It can be seen that the computation complexity of the centralized algorithm rapidly increases with the increase of the cache capacity Q, while the computation complexity of the distributed algorithm increases very slowly with the cache capacity Q. This indicates that the cache capacity has a greater impact on the computation complexity of the centralized algorithm rather than the distributed algorithm, since more elements are added greedily and more iterations are processed in the centralized algorithm when the cache capacity Q is increased. When applying the distributed algorithm, the cache capacity is a parameter which only adjusts the value of the messages during iterations. It does not change the factor graph model, and hence may not cause a significant impact on its computation complexity.

VII. Conclusions

In this work, we studied the cache placement problem in Fog-RANs, by taking into account different file preferences and diverse transmission opportunities for each user. We developed transmission aware cache placement strategies in both centralized and distributed operation modes of Fog-RANs. In the centralized mode, a low-complexity centralized greedy algorithm was proposed to achieve a suboptimal solution within a constant factor to the optimum using submodular optimization techniques. In the distributed mode, a low-complexity belief propagation based distributed algorithm was proposed to place files at the BSs based on locally collected information. Each BS run computations and exchange very few messages

with its neighboring BSs iteratively until convergence. By simulations, we showed that both of the proposed algorithms can not only improve the users' cache hit probability but also provide more flexible cooperative transmission opportunities for the users. As a result, our proposed centralized and distributed cache placement algorithms can significantly improve the file delivery performance by providing cooperative transmission opportunities for mobile users to the maximum extent. It was also shown that the distributed cache placement algorithm can achieve an average delay performance comparable to the centralized cache placement algorithm while spending much less calculations in each individual BS.

Appendix

A. Proof of Theorem 1

In the scenario when file f_n has been cached in one or multiple serving BSs of user u_k, i.e., $\sum_{a_m \in \mathcal{A}_k} x_{nm} \neq 0$, the associated BSs can transmit to user u_k with rate $R_{nk}(\boldsymbol{X}, i)$ (c.f. (1)-(2)) by applying some specific transmission scheme. Since the channel coefficients $h_{km}(i)$ are i.i.d. across the time slots $\{i\}$, the file delivery rates $R_{nk}(\boldsymbol{X}, i)$ are i.i.d. random variables. Hence, the stopping time of completing the transmission of file f_n, $T_{nk}^*(\boldsymbol{X})$ given by (3), is also a random variable. Based on the definition of channel capacity, we have $R_{nk}(\boldsymbol{X}, i) \geq 0$ for $i = 1, 2, \cdots, T_{nk}^*(\boldsymbol{X})$. According to Wald's Equation in martingale theory [31], we have

$$\mathbb{E}_{\boldsymbol{h}} \left\{ \sum_{i=1}^{T_{nk}^*(\boldsymbol{X})} R_{nk}(\boldsymbol{X}, i) \right\} \qquad (27)$$
$$= \mathbb{E}_{\boldsymbol{h}} \left\{ T_{nk}^*(\boldsymbol{X}) \right\} \cdot \mathbb{E}_{\boldsymbol{h}} \left\{ R_{nk}(\boldsymbol{X}) \right\} = \frac{|f_n|}{\Delta t}.$$

Therefore, the average download delay is expressed as

$$\bar{D}_{nk}(\boldsymbol{X}) = \mathbb{E}_{\boldsymbol{h}} \left\{ T_{nk}^*(\boldsymbol{X}) \cdot \Delta t \right\} = \frac{|f_n|}{\mathbb{E}_{\boldsymbol{h}} \left\{ R_{nk}(\boldsymbol{X}) \right\}}, \qquad (28)$$

when file f_n is cached in the associated BSs with $\sum_{a_m \in \mathcal{A}_k} x_{nm} \neq 0$. When $\sum_{a_m \in \mathcal{A}_k} x_{nm} = 0$, file f_n has not been cached in any serving BS of user u_k. The BSs $\mathcal{A}_k'$ download this file from the content server by the backhaul link and then transmit to user u_k over the wireless channel. Accordingly, the average delay can be estimated by $\bar{D}_{nk}(\boldsymbol{X}) = D_{nk} + \frac{|f_n|}{\mathbb{E}_{\boldsymbol{h}}\{R_{nk}(\boldsymbol{X}_k)\}}$, where D_{nk} is the extra delay of file delivery from the content server to the serving BSs $\mathcal{A}_k'$, and $R_{nk}(\boldsymbol{X}_k)$ is the data rate at which the BSs $\mathcal{A}_k'$ transmit file f_n to user u_k over wireless channel. Here, $\boldsymbol{X}_k$ is an equivalent caching strategy indicating that file f_n can be downloaded from the BSs $\mathcal{A}_k'$ by user u_k. Thus, the average delay $\bar{D}_{nk}(\boldsymbol{X})$ is established in (5).

B. Proof of Theorem 2

From Theorem 1, the average delay of downloading file f_n for user u_k presented in (5) can also be expressed as

$$\bar{D}_{nk}(\mathcal{X}) = \begin{cases} \frac{|f_n|}{R_{nk}(\mathcal{X})}, & \sum_{m=1}^{M} x_{nm} \neq 0, \\ D_{nk} + \frac{|f_n|}{\bar{R}_{nk}(\mathcal{X}_k)}, & \text{otherwise}, \end{cases} \qquad (29)$$

where $\bar{R}_{nk}(\mathcal{X}) = \mathbb{E}\{B\log(1 + Y_{nk}(\mathcal{X}))\}$ with $Y_{nk}(\mathcal{X}) = \sum_{m=1}^{M} |h_{km}|^2 x_{nm} \text{SINR}_m$ representing the received SINR.

10

We will show that the average delay $\tilde{D}_{nk}(\mathcal{X}) = -\bar{D}_{nk}(\mathcal{X})$ is a monotone submodular function.

Let $\mathcal{X} \subseteq \mathcal{X}' \in \mathcal{I}$, and $s \in \mathcal{S} \setminus \mathcal{X}'$. The incidence vectors for $\mathcal{X}$ and $\mathcal{X}'$ are denoted by $\boldsymbol{X} = [x_{nm}]$ and $\boldsymbol{X}' = [x'_{nm}]$, respectively. If $s \neq f_n^{(m)}$ for any $m \in \mathcal{A}_k$, we have $\tilde{D}_{nk}(\mathcal{X} \cup \{s\}) - \tilde{D}_{nk}(\mathcal{X}) = \tilde{D}_{nk}(\mathcal{X}' \cup \{s\}) - \tilde{D}_{nk}(\mathcal{X}') = 0$. We then consider the case when $s = f_n^{(m^*)}$ for any $m^* \in \mathcal{A}_k$.

Case I: $\mathcal{X} = \mathcal{X}' \in \mathcal{I}$ and $\sum_{m \in \mathcal{A}_k} x_{nm} = \sum_{m \in \mathcal{A}_k} x'_{nm}$

In this case, $s = \emptyset \in \mathcal{X}' \setminus \mathcal{X}$ and $\bar{D}_{nk}(\mathcal{X}) = \bar{D}_{nk}(\mathcal{X}')$. Hence, we have $\tilde{D}_{nk}(\mathcal{X} \cup \{s\}) - \tilde{D}_{nk}(\mathcal{X}) = \tilde{D}_{nk}(\mathcal{X}' \cup \{s\}) - \tilde{D}_{nk}(\mathcal{X}') = 0$.

Case II: $\mathcal{X} \subseteq \mathcal{X}' \in \mathcal{I}$ and $0 < \sum_{m \in \mathcal{A}_k} x_{nm} < \sum_{m \in \mathcal{A}_k} x'_{nm}$

According to the definition of $\bar{R}_{nk}(\mathcal{X})$, we have $\bar{R}_{nk}(\mathcal{X} \cup \{s\}) = \mathbb{E}\{B \log(1 + Y_{nk}(\mathcal{X}) + |h_{km^*}|^2 \text{SINR}_{m^*})\}$. Hence, $\bar{R}_{nk}(\mathcal{X}) < \bar{R}_{nk}(\mathcal{X}')$ and $\bar{R}_{nk}(\mathcal{X} \cup \{s\}) < \bar{R}_{nk}(\mathcal{X}' \cup \{s\})$ naturally hold due to $\sum_{m=1}^M x_{nm} < \sum_{m=1}^M x'_{nm}$ and $Y_{nk}(\mathcal{X}) < Y_{nk}(\mathcal{X}')$. The gap between $\tilde{D}_{nk}(\mathcal{X} \cup \{s\})$ and $\tilde{D}_{nk}(\mathcal{X})$ satisfies

$$\tilde{D}_{nk}(\mathcal{X} \cup \{s\}) - \tilde{D}_{nk}(\mathcal{X})$$
$$= \frac{|f_n|}{\bar{R}_{nk}(\mathcal{X})\bar{R}_{nk}(\mathcal{X} \cup \{s\})} \mathbb{E}\left\{ B \log\left(1 + \frac{|h_{km^*}|^2 \text{SINR}_{m^*}}{1 + Y_{nk}(\mathcal{X}')}\right)\right\}$$
$$\overset{(a)}{>} \frac{|f_n|}{\bar{R}_{nk}(\mathcal{X}')\bar{R}_{nk}(\mathcal{X}' \cup \{s\})} \mathbb{E}\left\{ B \log\left(1 + \frac{|h_{km^*}|^2 \text{SINR}_{m^*}}{1 + Y_{nk}(\mathcal{X}')}\right)\right\}$$
$$\overset{(b)}{>} \frac{|f_n|}{\bar{R}_{nk}(\mathcal{X}')\bar{R}_{nk}(\mathcal{X}' \cup \{s\})} \mathbb{E}\left\{ B \log\left(1 + \frac{|h_{km^*}|^2 \text{SINR}_{m^*}}{1 + Y_{nk}(\mathcal{X}')}\right)\right\}$$
$$= \tilde{D}_{nk}\left(\mathcal{X}' \cup \{s\}\right) - \tilde{D}_{nk}\left(\mathcal{X}'\right),$$

where the inequality (a) comes from $\bar{R}_{nk}(\mathcal{X}) \leq \bar{R}_{nk}(\mathcal{X}')$ and $\bar{R}_{nk}(\mathcal{X} \cup \{s\}) \leq \bar{R}_{nk}(\mathcal{X}' \cup \{s\})$, and the inequality (b) holds since $Y_{nk}(\mathcal{X}) < Y_{nk}(\mathcal{X}')$ and $B \log\left(1 + \frac{|h_{km^*}|^2 \text{SINR}_{m^*}}{1 + Y_{nk}(\mathcal{X})}\right) > B \log\left(1 + \frac{|h_{km^*}|^2 \text{SINR}_{m^*}}{1 + Y_{nk}(\mathcal{X}')}\right)$.

Case III: $\mathcal{X} \subseteq \mathcal{X}' \in \mathcal{I}$ and $0 = \sum_{m \in \mathcal{A}_k} x_{nm} < \sum_{m \in \mathcal{A}_k} x'_{nm}$

We have $\tilde{D}_{nk}(\mathcal{X} \cup \{s\}) - \tilde{D}_{nk}(\mathcal{X}) = D_{nk} + \frac{|f_n|}{\bar{R}_{nk}(\mathcal{X}_k)} - \frac{|f_n|}{\bar{R}_{nk}(\{s\})}$. The following inequality

$$\tilde{D}_{nk}(\mathcal{X} \cup \{s\}) - \tilde{D}_{nk}(\mathcal{X}) = D_{nk} + \frac{|f_n|}{\bar{R}_{nk}(\mathcal{X}_k)} - \frac{|f_n|}{\bar{R}_{nk}(\{s\})}$$
$$> \frac{|f_n|}{\bar{R}_{nk}(\mathcal{X}')} - \frac{|f_n|}{\bar{R}_{nk}(\mathcal{X}' \cup \{s\})} = \tilde{D}_{nk}\left(\mathcal{X}' \cup \{s\}\right) - \tilde{D}_{nk}\left(\mathcal{X}'\right)$$

is satisfied, since $D_{nk} + \frac{|f_n|}{\bar{R}_{nk}(\mathcal{X}_k)} > \frac{|f_n|}{\bar{R}_{nk}(\mathcal{X}')}$ and $\frac{|f_n|}{\bar{R}_{nk}(\{s\})} < \frac{|f_n|}{\bar{R}_{nk}(\mathcal{X}' \cup \{s\})}$. In this case, we still get $\tilde{D}_{nk}(\mathcal{X} \cup \{s\}) - \tilde{D}_{nk}(\mathcal{X}) > \tilde{D}_{nk}\left(\mathcal{X}' \cup \{s\}\right) - \tilde{D}_{nk}\left(\mathcal{X}'\right)$.

Combining the above three cases, we have

$$\tilde{D}_{nk}(\mathcal{X} \cup \{s\}) - \tilde{D}_{nk}(\mathcal{X}) \geq \tilde{D}_{nk}\left(\mathcal{X}' \cup \{s\}\right) - \tilde{D}_{nk}\left(\mathcal{X}'\right). \tag{30}$$

Meanwhile, it is trivial to show that since $\bar{R}_{nk}(\mathcal{X}) \leq \bar{R}_{nk}(\mathcal{X}')$, we have $\tilde{D}_{nk}(\mathcal{X}) \leq \tilde{D}_{nk}(\mathcal{X}')$ for any $\mathcal{X} \subseteq \mathcal{X}'$. Therefore, $\tilde{D}_{nk}(\mathcal{X})$ is a monotone submodular function. In the above discussion, cooperative beamforming is applied as a candidate transmission scheme to demonstrate the monotone

submodular property of the average delay function. In fact, this property holds for any candidate transmission scheme.

C. Basics of the Message Passing Procedure

We briefly introduce the factor graph model and the max-product algorithm. A factor graph is a bipartite graph which consists of I variable nodes $\{\mu_1, \cdots, \mu_I\}$ and J function nodes $\{F_1, \cdots, F_J\}$. Let Γ_i^μ and Γ_j^F denote the set of indices of the neighboring function nodes of a variable node μ_i and that of the neighboring variable nodes of a function node F_j, respectively. Max-product is a belief propagation algorithm based on the factor graph model, which is widely applied to find the optimum of the global function taking the form as $F(\boldsymbol{\mu}) = \prod_{j=1}^J F_j(\mu_{\Gamma_j^F})$ in a distributed manner. A comprehensive tutorial can be found in [27].

In each iteration, each variable node sends one updated message to one of its neighboring function nodes and receives one updated message from this node. According to the max-product algorithm [27], the message from a variable node μ_i to a function node F_j, i.e., $m_{\mu_i \to F_j}^t(x)$, is updated as

$$m_{\mu_i \to F_j}^{t+1}(x) = \prod_{l \in \Gamma_i^\mu \setminus \{j\}} m_{F_l \to \mu_i}^t(x), \tag{31}$$

which collects all the beliefs on the value of $\mu_i = x$ from the neighboring function nodes F_l ($l \in \Gamma_i^\mu \setminus \{j\}$) except F_j. The message from a function node F_j to a variable node μ_i, i.e., $m_{F_j \to \mu_i}^t(x)$, is updated as

$$m_{F_j \to \mu_i}^{t+1}(x) = \max_{\Gamma_j^F \setminus \{i\}} \left\{ F_j(\boldsymbol{X}) \prod_l m_{\mu_l \to F_j}^t(x_l) \right\}, \tag{32}$$

which achieves the maximization of the product of the local function $F_j(\boldsymbol{X})$ and incident messages over configurations in $\Gamma_j^F \setminus \{i\}$.

D. Proof of Theorem 4

By substituting (20) into (31), we can easily obtain the practical message $\alpha_{i \to j}^t$ as given by (21).

From (32), the derivation of the message $\beta_{j \to i}^t$ involves one maximization operation over all possible values of $\{\mu_l = x_l\}$ ($l \in \Gamma_j^F \setminus \{i\}$). Then, we discuss the message $\beta_{j \to i}^t$ in the cases when $F_j \doteq \eta_{nk}$ and $F_j \doteq g_m$, respectively.

Case I: Derivation of $\beta_{j \to i}^t$ for $F_j \doteq \eta_{nk}$

By substituting the average delay (such as the metric presented in (5)) into (32), the message $m_{F_j \to \mu_i}^{t+1}(1)$ with $F_j = \eta_{nk}$ and $\mu_i = 1$ can be represented as

$$m_{F_j \to \mu_i}^{t+1}(1) = \max_{E_i^1} \left\{ \exp(-p_{nk} \bar{D}_{nk}(\boldsymbol{X}^{(1)})) \prod_{l \in E_i^1} \left(\frac{m_{\mu_l \to F_j}^t(1)}{m_{\mu_l \to F_j}^t(0)} \right) \right\}$$
$$\times \prod_{l \in \Gamma_j^F \setminus \{i\}} m_{\mu_l \to F_j}^t(0), \tag{33}$$

where $E_i^1 \subseteq \Gamma_j^F \setminus \{i\}$ is a subset of the index set $\Gamma_j^F \setminus \{i\}$ such that its associated elements in $\boldsymbol{X}^{(1)}$ are equal to one, i.e., $\mu_l = 1$ for all $l \in E_i^1 \cup \{i\}$, while $\mu_l = 0$ for all $l \in \Gamma_j^F \setminus \{i\} \setminus E_i^1$. Similarly, we can compute the message $m_{F_j \to \mu_i}^{t+1}(0)$ as

$$m_{F_j\to\mu_i}^{t+1}(0) = \max_{E_i^2}\left\{\exp(-p_{nk}\bar{D}_{nk}(\boldsymbol{X}^{(0)}))\prod_{l\in E_i^2}\left(\frac{m_{\mu_l\to F_j}^t(1)}{m_{\mu_l\to F_j}^t(0)}\right)\right\}$$
$$\times\prod_{l\in\Gamma_j^F\setminus\{i\}}m_{\mu_l\to F_j}^t(0)\tag{34}$$

where $E_i^2\subseteq\Gamma_j^F\setminus\{i\}$ is also a subset of the index set $\Gamma_j^F\setminus\{i\}$ such that its associated elements in $\boldsymbol{X}^{(0)}$ are equal to one, while the other elements are zero with $\mu_l=0$ for all $l\in\Gamma_j^F\setminus E_i^2$. From (33) and (34), the message $\beta_{j\to i}^{t+1}$ can be expressed as

$$\beta_{j\to i}^{t+1} = \max_{E_i^1}\left\{(-p_{nk}\bar{D}_{nk}(\boldsymbol{X}^{(1)}))+\sum_{l\in E_i^1}\alpha_{l\to j}^t\right\}$$
$$-\max_{E_i^2}\left\{(-p_{nk}\bar{D}_{nk}(\boldsymbol{X}^{(0)}))+\sum_{l\in E_i^2}\alpha_{l\to j}^t\right\},\tag{35}$$
$$= p_{nk}\left(\bar{D}_{nk}(\boldsymbol{X}_i^{(0)})-\bar{D}_{nk}(\boldsymbol{X}_i^{(1)})\right),$$

where $\boldsymbol{X}_i^{(0)}$ and $\boldsymbol{X}_i^{(1)}$ are set as caching vectors by selecting the variable nodes $\{\mu_l\}$ with positive $\alpha_{l\to j}^t$, i.e., $l\in E_i^+ = \{i'\in\Gamma_j^F\setminus\{i\}|\alpha_{i'\to j}^t>0\}$, and assigning their associated elements to one. Thus, we have $\mu_l\doteq x_{nm}=1$ for all $l\in E_i^+$ in $\boldsymbol{X}_i^{(0)}$ and $\mu_l\doteq x_{nm}=1$ for all $l\in E_i^+\cup\{i\}$ in $\boldsymbol{X}_i^{(1)}$. This means that each function node F_j should select its neighboring variable nodes μ_l with positive input message $\alpha_{l\to j}^t$ and then calculate the delay gap between $\bar{D}_{nk}(\boldsymbol{X}_i^{(0)})$ and $\bar{D}_{nk}(\boldsymbol{X}_i^{(1)})$.

Case II: Derivation of $\beta_{j\to i}^t$ for $F_j\doteq g_m$

By substituting the constraint function into (32), the message $m_{F_j\to\mu_i}^{t+1}(1)$ when $F_j\doteq g_m$ can be represented as

$$m_{F_j\to\mu_i}^{t+1}(1) = \max_{E_i^3}\left\{g_m(\boldsymbol{X}^{(1)})\prod_{l\in E_i^3}\left(\frac{m_{\mu_l\to F_j}^t(1)}{m_{\mu_l\to F_j}^t(0)}\right)\right\}$$
$$\times\prod_{l\in\Gamma_j^F\setminus\{i\}}m_{\mu_l\to F_j}^t(0),\tag{36}$$

where E_i^3 is a subset of the index set $\Gamma_j^F\setminus\{i\}$ and $|E_i^3|\le Q_m-1$. This means that to satisfy the cache capacity constraint, there exist at most Q_m-1 neighboring variable nodes $\{\mu_l\}$ with $\mu_l=1$ $(l\in E_i^3)$ except the variable node $\mu_i=1$. Similarly, we can compute the message $m_{F_j\to\mu_i}^{t+1}(0)$ when $F_j\doteq g_m$ as

$$m_{F_j\to\mu_i}^{t+1}(0) = \max_{E_i^4}\left\{g_m(\boldsymbol{x}^{(0)})\prod_{l\in E_i^4}\left(\frac{m_{\mu_l\to F_j}^t(1)}{m_{\mu_l\to F_j}^t(0)}\right)\right\}$$
$$\times\prod_{l\in\Gamma_j^F\setminus\{i\}}m_{\mu_l\to F_j}^t(0)\tag{37}$$

where E_i^4 is a subset of the index set $\Gamma_j^F\setminus\{i\}$ and $|E_i^4|\le Q_m$. Since $\mu_i=0$, there exist at most Q_m neighboring variable nodes $\{\mu_l\}$ $(l\in E_i^4)$ with $\mu_l=1$ to satisfy the cache capacity constraint. From (36) and (37), the message ratio of $m_{F_j\to\mu_i}^{t+1}(1)$ and $m_{F_j\to\mu_i}^{t+1}(0)$ in the logarithmic domain can be expressed as

$$\beta_{j\to i}^{t+1} = \max_{E_i^3}\left\{\sum_{l\in E_i^3}\alpha_{l\to j}^t\right\}-\max_{E_i^4}\left\{\sum_{l\in E_i^4}\alpha_{l\to j}^t\right\}.\tag{38}$$

By sorting the messages $\{\alpha_{l\to j}^t\}$ $(\forall l\in\Gamma_j^F\setminus\{i\})$ in the decreasing order as $\alpha_{l\to j}^{(1)}, \alpha_{l\to j}^{(2)}, \cdots, \alpha_{l\to j}^{(Q_m-1)}, \cdots$, we can further simplify $\beta_{j\to i}^{t+1}$ as

$$\beta_{j\to i}^{t+1} = \begin{cases}\min\{0,-\alpha_{l\to j}^{(Q_m)}\}, & \text{if }\alpha_{l\to j}^{(Q_m-1)}\ge 0,\\ 0, & \text{otherwise,}\end{cases}\tag{39}$$

which is exactly equal to $\min\{0,-\alpha_{l\to j}^{(Q_m)}\}$, as given by (23).

REFERENCES

[1] J. Liu, B. Bai, J. Zhang, and K. B. Letaief, "Content caching at the wireless network edge: A distributed algorithm via belief propagation," in *Proc. IEEE ICC*, Kuala Lumpur, Malaysia, May 2016.

[2] M. Chiang, "Fog networking: An overview on research opportunities," Jan. 2016. [Online]. Available: http://arxiv.org/ftp/arxiv/papers/1601/1601.00835.pdf

[3] S.-H. Park, O. Simeone, and S. Shamai (Shitz), "Joint optimization of cloud and edge processing for fog radio access networks," Jan. 2016. [Online]. Available: http://arxiv.org/pdf/1601.02460v1.pdf

[4] Y. Shi, J. Zhang, K. B. Letaief, B. Bai, and W. Chen, "Large-scale convex optimization for ultra-dense cloud-RAN," *IEEE Wireless Commun.*, vol. 22, no. 3, pp. 84–91, Jun. 2015.

[5] S. Borst, V. Gupta, and A. Walid, "Distributed caching algorithms for content distribution networks," in *Proc. IEEE INFOCOM*, Mar. 2010, pp. 1–9.

[6] N. Golrezaei, A. F. Molisch, and A. G. Dimakis, "Base-station assisted device-to-device communications for high-throughput wireless video networks," in *Proc. IEEE ICC*, Jun. 2012, pp. 7077–7081.

[7] M. A. Maddah-Ali and U. Niesen, "Fundamental limits of caching," *IEEE Trans. Inf. Theory*, vol. 60, no. 5, pp. 2856–2867, May 2014.

[8] N. Golrezaei, K. Shanmugam, A. G. Dimakis, A. F. Molisch, and G. Caire, "FemtoCaching: Wireless video content delivery through distributed caching helpers," in *Proc. IEEE INFOCOM*, Mar. 2012, pp. 1107–1115.

[9] X. Peng, J.-C. Shen, J. Zhang, and K. B. Letaief, "Backhaul-aware caching placement for wireless networks," in *Proc. IEEE Globecom*, San Diego, CA, Dec. 2015.

[10] E. Baştuğ, M. Bennis, M. Kountouris, and M. Debbah, "Cache-enabled small cell networks: Modeling and tradeoffs," *EURASIP J. Wireless Commun.*, vol. 2015, no. 1, p. 41, Feb. 2015. [Online]. Available: http://jwcn.eurasipjournals.com/content/2015/1/41/abstract

[11] M. Ji, G. Caire, and A. F. Molisch, "Optimal throughput-outage trade-off in wireless one-hop caching networks," in *Proc. IEEE International Symposium on Information Theory Proceedings (ISIT)*, Jul. 2013, pp. 1461–1465.

[12] ——, "Wireless device-to-device caching networks: Basic principles and system performance," *IEEE J. Sel. Areas in Commun.*, vol. 34, no. 1, pp. 176–189, Jan. 2015.

[13] S.-W. Jeon, S.-N. Hong, M. Ji, G. Caire, and A. F. Molisch, "Wireless multihop device-to-device caching networks," Nov. 2015. [Online]. Available: http://arxiv.org/abs/1511.02574

[14] A. Liu and V. Lau, "On the improvement of scaling laws for wireless ad hoc networks with physical layer caching," in *Proc. IEEE ISIT*, Jun. 2015, pp. 161–165.

[15] M. Tao, E. Chen, H. Zhou, and W. Yu, "Content-centric sparse multicast beamforming for cache-enabled cloud RAN," *IEEE Trans. Wireless Commun.*, vol. 15, no. 9, pp. 6118–6131, Sep. 2016.

[16] B. Zhou, Y. Cui, and M. Tao, "Stochastic content-centric multicast scheduling for cache-enabled heterogeneous cellular networks," *IEEE Trans. Wireless Commun.*, vol. 15, no. 9, pp. 1536–1276, Sep. 2016.

[17] U. Niesen and M. A. Maddah-Ali, "Coded caching with nonuniform demands," in *Proc. IEEE INFOCOM WKSHPS*, April 27-May 2 2014, pp. 221–226.

[18] M. A. Maddah-Ali and U. Niesen, "Decentralized coded caching attains order-optimal memory-rate tradeoff," *IEEE/ACM Trans. Network.*, vol. 23, no. 4, pp. 1029–1040, Aug. 2015.

[19] N. Karamchandani, U. Niesen, M. A. Maddah-Ali, and S. Diggavi, "Hierarchical coded caching," in *Proc. IEEE ISIT*, Jun. 2014, pp. 2142–2146.

[20] H. Ahlehagh and S. Dey, "Video-aware scheduling and caching in the radio access network," *IEEE/ACM Trans. Network.*, vol. 22, no. 5, pp. 1444–1462, Oct. 2014.

[21] A. Abboud, E. Baştuğ, K. Hamidouche, and M. Debbah, "Distributed caching in 5G networks: An alternating direction method of multipliers approach," in *Proc. IEEE International Workshop on Signal Processing Advances in Wireless Communications (SPAWC), Stockholm, Sweden*, June 28-July 1 2015.

[22] R. Wang, X. Peng, J. Zhang, and K. B. Letaief, "Mobility-aware caching for content-centric wireless networks: Modeling and methodology," *IEEE Commun. Mag.*, vol. 54, no. 8, pp. 77–83, Aug. 2016.

[23] K. Poularakis, G. Iosifidis, and L. Tassiulas, "Approximation algorithms for mobile data caching in small cell networks," *IEEE Trans. Commun.*, vol. 62, no. 10, pp. 3665–3677, Oct. 2014.

[24] M. Dehghan, A. Seetharam, B. Jiang, T. He, T. Salonidis, J. Kurose, D. Towsley, and R. Sitaraman, "On the complexity of optimal routing and content caching in heterogeneous networks," in *Proc. INFOCOM*, April 26-May 1 2015.

[25] L. Breslau, P. Cao, L. Fan, G. Phillips, and S. Shenker, "Web caching and Zipf-like distributions: Evidence and implications," in *Proc. IEEE INFOCOM*, Mar. 1999, pp. 126–134.

[26] A. Schrijver, *Combinatorial optimization: Polyhedra and efficiency*. Berlin: Springer, 2003.

[27] F. R. Kschischang, B. J. Frey, and H.-A. Loeliger, "Factor graphs and the sum-product algorithm," *IEEE Trans. Inf. Theory*, vol. 47, no. 2, pp. 498–519, Feb. 2001.

[28] E. Baştuğ, M. Bennis, and M. Debbah, "A transfer learning approach for cache-enabled wireless networks," in *Proc. 13th International Symposium on Modeling and Optimization in Mobile, Ad Hoc, and Wireless Networks (WiOpt)*, May 2015, pp. 161–166.

[29] B. N. Bharath, K. G. Nagananda, and H. V. Poor, "A learning-based approach to caching in heterogenous small cell networks," Aug. 2015. [Online]. Available: http://arxiv.org/abs/1508.03517

[30] R. Mudumbai, G. Barriac, and U. Madhow, "On the feasibility of distributed beamforming in wireless networks," *IEEE Trans. Wireless Commun.*, vol. 6, no. 5, pp. 1754–1763, May 2007.

[31] David Williams, *Probability with Martingale*. Cambridge University Press, 1991.

[32] K. Shanmugam, N. Golrezaei, A. G. Dimakis, A. F. Molisch, and G. Caire, "FemtoCaching: Wireless content delivery through distributed caching helpers," *IEEE Trans. Inf. Theory*, vol. 59, no. 12, pp. 8402–8413, Dec. 2013.

[33] J. Leskovec, A. Krause, C. Guestrin, C. Faloutsos, J. VanBriesen, and N. Glance, "Cost-effective outbreak detection in networks," in *Proc. 13th ACM Int. Conf. on Knowledge Discovery and Data Mining (KDD)*, 2007, pp. 420–429.